Direct Inclusion of Proximity-Effect Losses in Two-Dimensional Time-Domain Finite-Element Simulation of Electrical Machines

Johan Gyselinck[1], Patrick Dular[2,3] Christophe Geuzaine[2] and Ruth V. Sabariego[2]

[1]Dept. of Bio-, Electro- and Mechanical Systems, Université Libre de Bruxelles, Belgium, E-mail: Johan.Gyselinck@ulb.ac.be
[2]Dept. of Electrical Engineering and Computer Science (ACE), University of Liége, Belgium
[3]Fonds de la Recherche Scientifique, F.R.S.-FNRS, Belgium

***Abstract* — This paper deals with eddy-current effects in the distributed winding of electrical machines, and in particular with the proximity effect and the associated losses. A previously proposed homogenization method for windings in two-dimensional (2D) time-domain finite-element (FE) models is shown to be applicable without additional computational cost, producing a precise estimate of the instantaneous proximity-effect losses. The method is illustrated by considering the conductors in a single stator slot of a 3kW induction motor. The brute-force model, with fine discretisation of each conductor, and the homogenized model yield macroscopic results that are very close to each other.**

I. INTRODUCTION

Multiturn windings in electromagnetic devices may be subjected to considerable skin and proximity effect [1]. Most often these effects are simply ignored in the resolution stage of the FE simulation, and the associated losses are estimated *a posteriori*. However, in some cases the behaviour of the device under study can be significantly altered by the eddy-current effects, and their direct inclusion in the FE modeling is required. As an alternative to the prohibitively expensive brute-force approach, which requires a fine discretization of each separate turn of the winding and associated electrical circuit equations, accurate frequency and time domain homogenization methods have recently been proposed in [2]. In the time-domain case, the additional computational cost depends on the frequency content of the application, and in particular on the conductor radius to skin depth ratio.

In the case of electrical machine windings, the latter ratio is generally sufficiently low so as to allow a simple implementation of the time-domain method, with furthermore negligible additional computational cost. This will be illustrated in the present paper by considering a 3kW induction motor [3].

II. EDDY-CURRENT EFFECT COEFFICIENTS

A complete eddy-current effect characterization of a winding (shape of the conductor cross-section, packing type and fill factor) can be carried out by means of a representative 2D FE model consisting of a central cell and a layer of cells around it [1][2]. See Fig. 1.

A. Frequency domain coefficients

We define the *reduced frequency* X as follows:

$$X \;=\; r/\delta \;=\; \sqrt{f}\cdot r\sqrt{\pi\sigma\mu_0}\,, \tag{1}$$

with $r = \sqrt{\mathcal{A}_c/\pi}$ the equivalent radius of the conductors ($\mathcal{A}_c$ being the conductor surface area), δ the penetration depth at frequency f or pulsation $\omega = 2\pi f$, σ the conductivity of the conductors, and $\mu_0 = 4\pi 10^{-7}$ H/m and $\nu_0 = 1/\mu_0$ their permeability and reluctivity.

Frequency-domain 2D FE calculations are carried out using the complex notation (symbols in bold, $\imath$ imaginary unit,

This work is partly supported by the Belgian Science Policy (IAP P6/21).

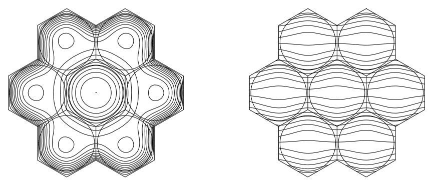

Fig. 1. Winding with conductors of circular cross-section and hexagonal packing: skin-effect flux pattern (left) and proximity-effect flux pattern (right)

* indicating the conjugate value) for the sinusoidal time variation. The classical magnetic vector potential formulation is adopted [4]. The same net current $\boldsymbol{I}$ is imposed in all conductors by means of electrical circuit equations, whereas the average induction $\boldsymbol{b}_{av}$ in the central cell can be imposed via the boundary conditions. This way skin effect and proximity effect can be separated as follows. A pure skin-effect excitation is obtained at the level of the central cell by imposing $\boldsymbol{a} = 0$ on the complete boundary (yielding $\boldsymbol{b}_{av} = 0$ thanks to the symmetry) and a unit net current ($\boldsymbol{I} = 1$ A) in all conductors (flux pattern in Fig. 1 left). By imposing a unit horizontal (or vertical) induction ($\boldsymbol{b}_{av} = 1$ T) through appropriate boundary condition and a zero net current ($\boldsymbol{I} = 0$), a pure proximity-effect excitation is effected (Fig. 1 right).

From these field solutions, obtained at a certain pulsation ω, the complex power $\boldsymbol{S}$ (in VA) absorbed by the central cell Ω_c is calculated by considering the local current density j and flux density b in the central cell Ω_c:

$$\boldsymbol{S} \;=\; P + \imath\, Q \;=\; \frac{l}{2}\int_{\Omega_c} (j^2/\sigma + \imath\,\omega\,\nu_0\, b^2)\, d\Omega\,, \tag{2}$$

with P and Q the active and reactive power, and $j^2/2 = \boldsymbol{j}\boldsymbol{j}^*/2$ and $b^2/2 = \boldsymbol{b}\boldsymbol{b}^*/2$ r.m.s.-values squared; l is the length along the third dimension (which can be arbitrarily taken to be 1 m). We can then define a complex skin effect impedance $\boldsymbol{Z}_{skin}$ (which replaces the DC resistance in the frequency-domain circuit equations) and a complex proximity-effect reluctivity $\boldsymbol{\nu}_{prox}$ (which replaces ν_0 in the field equations) [2]. In multi-layer windings (as in electrical machines), the skin-effect losses are normally negligible compared to the proximity-effect losses. We will therefore focus on the latter effect and losses in the remaining of this paper.

The complex proximity-effect reluctivity $\boldsymbol{\nu}_{prox}(X)$, at reduced frequency X, can be written in terms of dimensionless coefficients $p_B(X)$ and $q_B(X)$:

$$\boldsymbol{\nu}_{prox} \;=\; \frac{Q + \imath\, P}{\frac{1}{2}\omega\, l\, b_{av}^2\, \mathcal{A}_c/\lambda} \;=\; \nu_0\left(q_B + \imath\, p_B\,\frac{\lambda X^2}{2}\right), \tag{3}$$

where the factor $\frac{\lambda X^2}{2}$ follows from the analytical expression for low-frequency proximity losses in a round conductor [1], and where λ is the fill factor of the winding and $\mathcal{A}_c/\lambda$ is the surface area of one cell.

Fig. 2 shows how these coefficients vary with λ and X (up to 4). The packing type, hexagonal or square, has little influence. The coefficients tend to 1 as the frequency tends to 0.

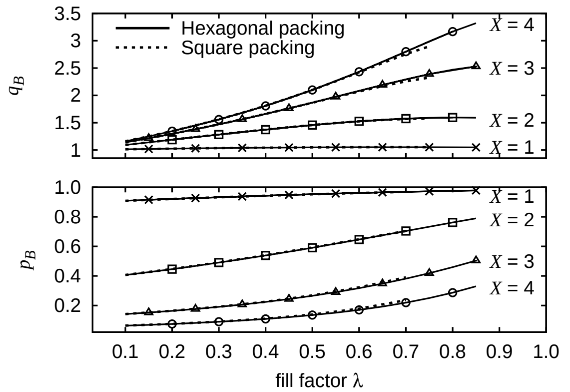

Fig. 2. Proximity effect coefficients q_B and p_B as a function of fill factor λ for different values of X

B. Time-domain approach for the proximity effect

The frequency-dependant reluctivity $\boldsymbol{\nu}_{prox}(X)$ of the homogenized winding can be translated into approximate time-domain equations by considering the homogenized magnetic induction $b(t)$ and a number of auxiliary (fictitious) induction components $b_2(t)$, $b_3(t)$, ... [2]. The simple algebraic constitutive law $h = \nu_0\, b$, with $h(t)$ the magnetic field, thus becomes a system of n first-order differential equations in terms of the n induction components. With $n = 3$, e.g., this system can be written as

$$\begin{bmatrix} h \\ 0 \\ 0 \end{bmatrix} = \nu_0 \begin{bmatrix} b \\ b_2 \\ b_3 \end{bmatrix} + \frac{\lambda\sigma r^2}{4} \begin{bmatrix} p_{11} & p_{12} & 0 \\ p_{12} & p_{22} & p_{23} \\ 0 & p_{23} & p_{33} \end{bmatrix} \frac{d}{dt} \begin{bmatrix} b \\ b_2 \\ b_3 \end{bmatrix} . \quad (4)$$

The symmetric tridiagonal dimensionless matrix in (4) is obtained using a fitting algorithm and considering the complex reluctivity $\boldsymbol{\nu}_{prox}(X)$ in the relevant frequency range $[0, X_{max}]$. The greater X_{max}, the more induction components are required to achieve good precision, and the greater the additional computation time. The case $n = 3$ corresponds to X_{max} equal to 4 [2].

In electrical machines, the relevant frequency range is much smaller, with normally X_{max} well below 1. The time-domain approximation, with $n = 1$, then becomes very simple:

$$h(t) = \nu_0\, b(t) + p_{11} \frac{\lambda\sigma r^2}{4} \frac{db}{dt}\,, \quad (5)$$

where p_{11} is pratically 1. This constitutive law is easy to account for in the FE equations. Indeed, the first term in the right-hand side of (5) gives the classical contribution to the FE stiffness matrix, whereas the second term leads to the following type of elemental contribution to the conductivity matrix (which is normally only due to so-called massive conductors in the FE domain [4]):

$$\int_{element} p_{11} \frac{\lambda\sigma r^2}{4} \operatorname{grad}\alpha_i \cdot \operatorname{grad}\alpha_j \, d\Omega\,, \quad (6)$$

where α_i and α_j are nodal basis functions.

III. APPLICATION TO A 3KW INDUCTION MOTOR

The homogenization method (with $n = 1$) is applied to one stator slot (out of 36) of a 4-pole 3kW cage induction motor. See [3] for simulation and experimental results, considering 4 different rotors: with either skewed and unskewed slots, and with either open or closed slots. One stator slot comprises 102 conductors (with $r = 0.3$ mm, $\lambda = 0.48$ considering the wound part of the slot, $\sigma = 6e7$ S/m). The fundamental 50 Hz current component ($X = 0.033$) produces negligible proximity effect. The first rotor slot harmonic is situated around 800 Hz ($X = 0.13$), with a current component up to 20% of the fundamental in case of unskewed slots [3]. Figure 3 shows the FE model (with imposed $\boldsymbol{a} = 0$ on the lower segment at the slot opening, and natural Neumann condition on the rest of the boundary) and flux patterns with the latter X-value. Fig. 4 shows that the additional proximity-effect losses are accurately calculated with the homogenization method ($n = 1$) up to $X = 0.5$ and above. In this X-range, the variation in inductance is seen to be negligible. More results and discussion will be supplied in the full paper.

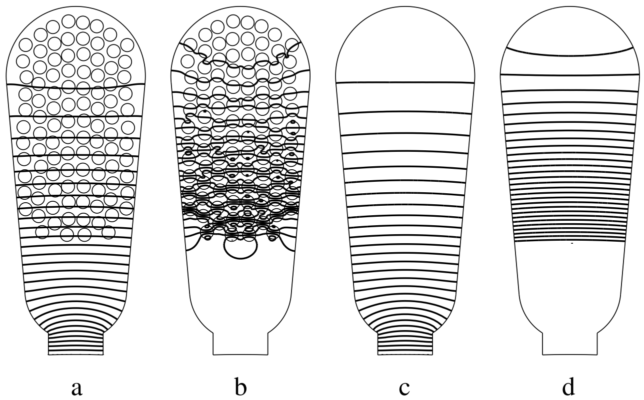

Fig. 3. Flux lines at $X = 0.13$ obtained with fine model (a and b) and with homogenized model (c and d), with flux component in phase with imposed unit current (a and c) and in quadrature (b and d)

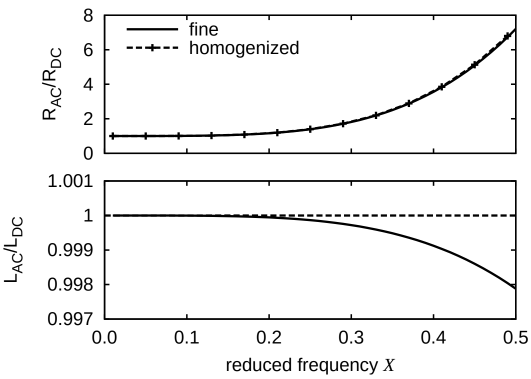

Fig. 4. Variation of joule losses and slot inductance (compared to DC value) with X

REFERENCES

[1] A. Podoltsev and B. Lebedev, “Analysis of effective resistance and eddy-current losses in multiturn winding of high-frequency magnetic components”, *IEEE Trans. on Magn.*, vol. 39, no. 1, pp. 539–548, January 2003.

[2] J. Gyselinck, R. Sabariego and P. Dular, “Time-domain homogenisation of windings in two-dimensional finite element models”, *IEEE Trans. on Magn.*, vol. 43, pp. 1297–1300, 2007.

[3] J. Gyselinck, L. Vandevelde and J. Melkebeek “Multi-slice FE modelling of electrical machines with skewed slots – the skew discretisation error”, *IEEE Trans. on Magn.*, vol. 37, pp. 3233–3237, 2001.

[4] P. Lombard and G. Meunier, “A general purpose method for electric and magnetic combined problems for 2D, axisymmetric and transient systems”, *IEEE Trans. on Magn.*, vol. 29, no. 2, pp. 1737–1740, March 1993.